remote sensing

MDPI

Review

The CYGNSS Mission: On-Going Science Team Investigations

Hugo Carreno-Luengo [1,*], Juan A. Crespo [2], Ruzbeh Akbar [3], Alexandra Bringer [4], April Warnock [5], Mary Morris [2] and Chris Ruf [1]

1 Climate and Space Sciences and Engineering Department, University of Michigan (UM), Ann Arbor, MI 48104, USA; cruf@umich.edu
2 Jet Propulsion Laboratory (JPL), California Institute of Technology, Pasadena, CA 91125, USA; juan.a.crespo@jpl.nasa.gov (J.A.C.); mary.g.morris@jpl.nasa.gov (M.M.)
3 Massachusetts Institute of Technology (MIT), Cambridge, MA 02139, USA; rakbar@mit.edu
4 Electrical and Computer Engineering, The Ohio State University, Columbus, OH 43210, USA; bringer.1@osu.edu
5 SRI International, Ann Arbor, MI 48105, USA; april.warnock@sri.com
* Correspondence: carreno@umich.edu; Tel.: +1-734-764-6561

Abstract: In 2012, the National Aeronautics and Space Administration (NASA) selected the CYclone Global Navigation Satellite System (CYGNSS) mission coordinated by the University of Michigan (UM) as a low-cost and high-science Earth Venture Mission. The CYGNSS mission was originally proposed for ocean surface wind speed estimation over Tropical Cyclones (TCs) using Earth-reflected Global Positioning System (GPS) signals, as signals of opportunity. The orbital configuration of each CYGNSS satellite is a circular Low Earth Orbit (LEO) with an altitude ~520 km and an inclination angle of ~35°. Each single Delay Doppler Mapping Instrument (DDMI) aboard the eight CYGNSS microsatellites collects forward scattered signals along four specular directions (incidence angle of the incident wave equals incidence angle of the reflected wave) corresponding to four different transmitting GPS spacecrafts, simultaneously. As such, CYGNSS allows one to sample the Earth's surface along 32 tracks simultaneously, within a wide range of the satellites' elevation angles over tropical latitudes. Following the Earth Science Division 2020 Senior Review, NASA announced recently it is extending the CYGNSS mission through 30 September 2023. The extended CYGNSS mission phase is focused on both ocean and land surface scientific investigations. In addition to ocean surface wind speed estimation, CYGNSS has also shown a significant ability to retrieve several geophysical parameters over land surfaces, such as Soil Moisture Content (SMC), Above Ground Biomass (AGB), and surface water extent. The on-going science team investigations are presented in this article.

Keywords: CYGNSS; GNSS-R; science investigations; ocean; land; atmosphere

Citation: Carreno-Luengo, H.; Crespo, J.A.; Akbar, R.; Bringer, A.; Warnock, A.; Morris, M.; Ruf, C. The CYGNSS Mission: On-Going Science Team Investigations. *Remote Sens.* **2021**, *13*, 1814. https://doi.org/10.3390/rs13091814

Academic Editor: Emanuele Santi

Received: 1 March 2021
Accepted: 1 May 2021
Published: 6 May 2021

1. Introduction

The CYGNSS Science Team [1–5] is composed of a wide variety of researchers, working in a collaborative and coordinated manner to further advance the use of CYGNSS for Global Navigation Satellite Systems Reflectometry (GNSS-R) Earth remote sensing [6–8].

GNSS-R is a type of L-band passive multi-bistatic radar, which uses the navigation spacecrafts which are in view as transmitters. GNSS-R provides global coverage, full temporal availability, and sampling of the Earth's surface over several tracks within a wide area up to ~1500 km. One potential disadvantage is the degraded spatial resolution under the incoherent scattering regime. The use of GNSS radio-navigation signals for Earth remote sensing has been investigated since it was originally proposed for mesoscale ocean altimetry by the European Space Agency (ESA) [9]. The first in-orbit proof-of-concept study was an experiment performed at the Jet Propulsion Laboratory (JPL) using the Space-borne Imaging Radar-C (SIR-C) on-board the Space Shuttle [10]. This experiment motivated the development of GNSS-R. At present, several GNSS-R space-borne studies have been

performed with several satellites, including United Kingdom (UK) Disaster Monitoring System-1 (DMC-1) [11], UK Techdemosat-1 (TDS-1) [12], Soil Moisture Active Passive (SMAP) [13], and the CYGNSS 8 microsatellites constellation [3] which is the first-ever operational GNSS-R mission.

The CYGNSS Science Team (Figure 1, Table 1) holds two Science Team meetings every year to coordinate such activities, and to share our most recent results. The last 2020 conference was held in UM (virtual conference) in June 2020 (Figure 1). This conference was structured along six different sessions covering all of our research topics: Session 1 (CYGNSS Mission Overview and Data Products I), Session 2 (CYGNSS Data Products II), Session 3 (Land Processes I), Session 4 (Land Processes II), Session 5 (Altimetry and Tropical Cyclones and Tropical Convection I), and Session 6 (Tropical Cyclones and Tropical Convection II). This article provides a synoptic overview of the meeting.

Table 1. Some key-members of the CYGNSS Science Team. The full list is available in [14].

Member	**Chris Ruf**
Home Institution	University of Michigan
CYGNSS Role	Principal Investigator
Areas	Earth environment remote sensing methods, instrumentation, atmosphere
Member	Mahta Moghaddam
Home Institution	University of Southern California
CYGNSS Role	Terrestrial Science Lead, Co-I
Areas	Inverse scattering, subsurface characterization, water resources
Member	Derek Posselt
Home Institution	Jet Propulsion Laboratory, California Institute of Technology
CYGNSS Role	Atmospheric Science Lead, Co-I
Areas	Clouds and precipitation, data assimilation, uncertainty quantification
Member	Ruzbeh Akbar
Home Institution	Massachusetts Institute of Technology
CYGNSS Role	Soil moisture sensor networks, calibration, and validation
Areas	Microwave remote sensing of Earth, hydrology, wireless sensor networks
Member	Alexandra Bringer
Home Institution	The Ohio State University
CYGNSS Role	CYGNSS Science Team member
Areas	Microwave remote sensing of the Earth, ocean and land applications
Member	Juan A. Crespo
Home Institution	Jet Propulsion Laboratory, California Institute of Technology
CYGNSS Role	Competed Science Team Member, CYGNSS ocean surface heat flux product
Areas	Extratropical cyclones & air-sea fluxes
Member	Mary Morris
Home Institution	Jet Propulsion Laboratory, California Institute of Technology
CYGNSS Role	CYGNSS Science Team member
Areas	Metereological and hydrological applications, Earth sciences
Member	April Warnock
Home Institution	SRI International
CYGNSS Role	CYGNSS Science Team member
Areas	Hydrology/storm surge modeling
Member	Hugo Carreno-Luengo
Home Institution	University of Michigan
CYGNSS Role	CYGNSS Science Team member
Areas	Surface scattering, Earth sciences

Figure 1. Zoom-derived photo of some Science Team members attending the June 2020 CYGNSS meeting.

2. Methodology, Results, and Discussions

2.1. Data Products

CYGNSS is within the NASA's Earth System Science Pathfinder (ESSP) program. The original goal of CYGNSS was to further advance extreme weather predictions with a focus on TCs inner core process studies. CYGNSS was designed to resolve the lack of accuracy with current TCs intensity forecasts, which lie in inadequate measurements and modeling of the inner core. The inaccurate measurements result from two main aspects:

- Traditional remote sensing techniques are blind to much of the inner core ocean surface when intense precipitation is in the eye wall and inner rain bands.
- Traditional high-inclination orbit and wide-swath surface wind imagers do not provide an enough temporal sampling of the dynamically evolving (genesis and rapid intensification) phases of the TCs life cycle.

CYGNSS was specifically designed to address these two limitations by combining the use of GNSS-R with the sampling properties of a constellation of eight microsatellites [15–19]. CYGNSS provides an unprecedented spatiotemporal resolution of the Earth's surface thanks to the multi-static nature of GNSS-R and the use of such a dense constellation of microsatellites. CYGNSS is the first operational GNSS-R mission launched into space, in 2016.

Since CYGNSS's launch in December 2016, various science data products (Figure 2) have been created, such as an expansion of its wind speed measurements, ocean surface heat flux measurements, and land observations [20]. These scientific data products expand CYGNSS's core mission beyond TCs observations and bolster its reach and influence within the Earth science community. The results presented here focus on some of these products that have been developed and published since launch. All CYGNSS data products available to the public are distributed by the Physical Oceanography Distributed Active Archive Center (PODAAC).

Session 1: CYGNSS Mission Overview and Data Products I

The current v2.1 CYGNSS mission science data products assume that the GPS transmit power is constant. The Climate Data Record (CDR) v1.0 was released in May 2020 to improve product performance. This is the most stable, and most accurate product currently available. Current v3.0 products incorporate real time monitoring of GPS power. At present, all eight CYGNSS spacecrafts are healthy and operating nominally. There was the open call "A.27 CYGNSS Competed Science Team" within NASA Research Opportunities in Space and Earth Science (ROSES) 2020 with the following research topics: Atmospheric River Generation and Development, Wetland Methane Emissions, Dynamic Inland Water Mask Development, Process, Coupling and Feedback Studies, and Weather and Storm Surge Data Assimilation Studies. This ROSES seeks to support the continued use of both the ocean and land data products through scientific investigations and end-user applications.

Several significant advances in ocean research activities were presented by the CYGNSS Science Team. By comparing the CYGNSS measured Mean-Square Slope (MSS) and modified Wave-Watch 3 (WW3) modeled MSS, it was shown that the mean MSS ratio has a dependence on both GPS Pseudo-Random Noise codes (PRNs) and CYGNSS Flight Models (FMs) (starboard and port antennas). A new end-to-end CYGNSS Level 1 calibration approach was proposed in [21] to: (1) improve the data quality of the CYGNSS Level 1 calibration and the Level 2 wind speed and MSS products; and (2) improve our understanding of the impacts of wind-wave and swell-wave on the GNSS-R ocean observations. The detailed performance assessments will be reported in the future. Sensitivity in CYGNSS data to wind direction was demonstrated by computing the kurtosis over areas in the glistening zone of different size and symmetry. CYGNSS raw Intermediate Frequency (IF) data processing at Institute of Space Sciences (ICE)—Institute of Space Studies of Catalonia (IEEC) demonstrated potential applications over land, inland water bodies, and in extreme events (e.g., hurricanes and floods) and regions of great geophysical interest (e.g., Himalayan glaciers). Finally, variational wind speed retrievals of uncalibrated CYGNSS data demonstrated a better response to high winds than the Advanced SCATterometer (ASCAT) radars and similar response as the Soil Moisture Ocean Salinity (SMOS) mission (Figure 3).

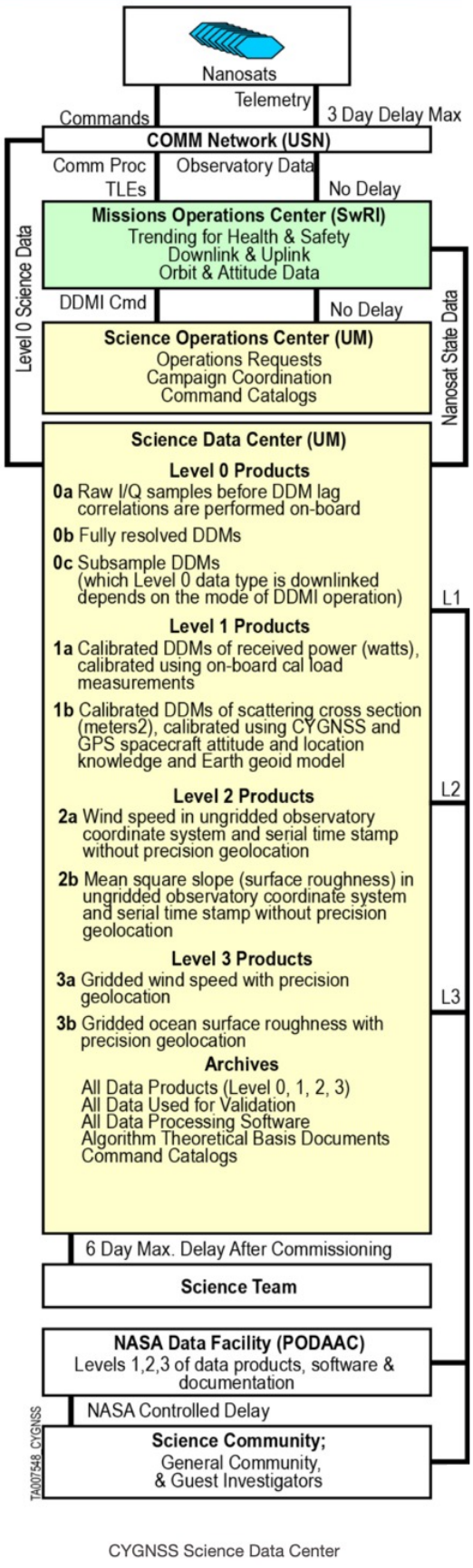

Figure 2. Data processing flow of the CYGNSS data products [19].

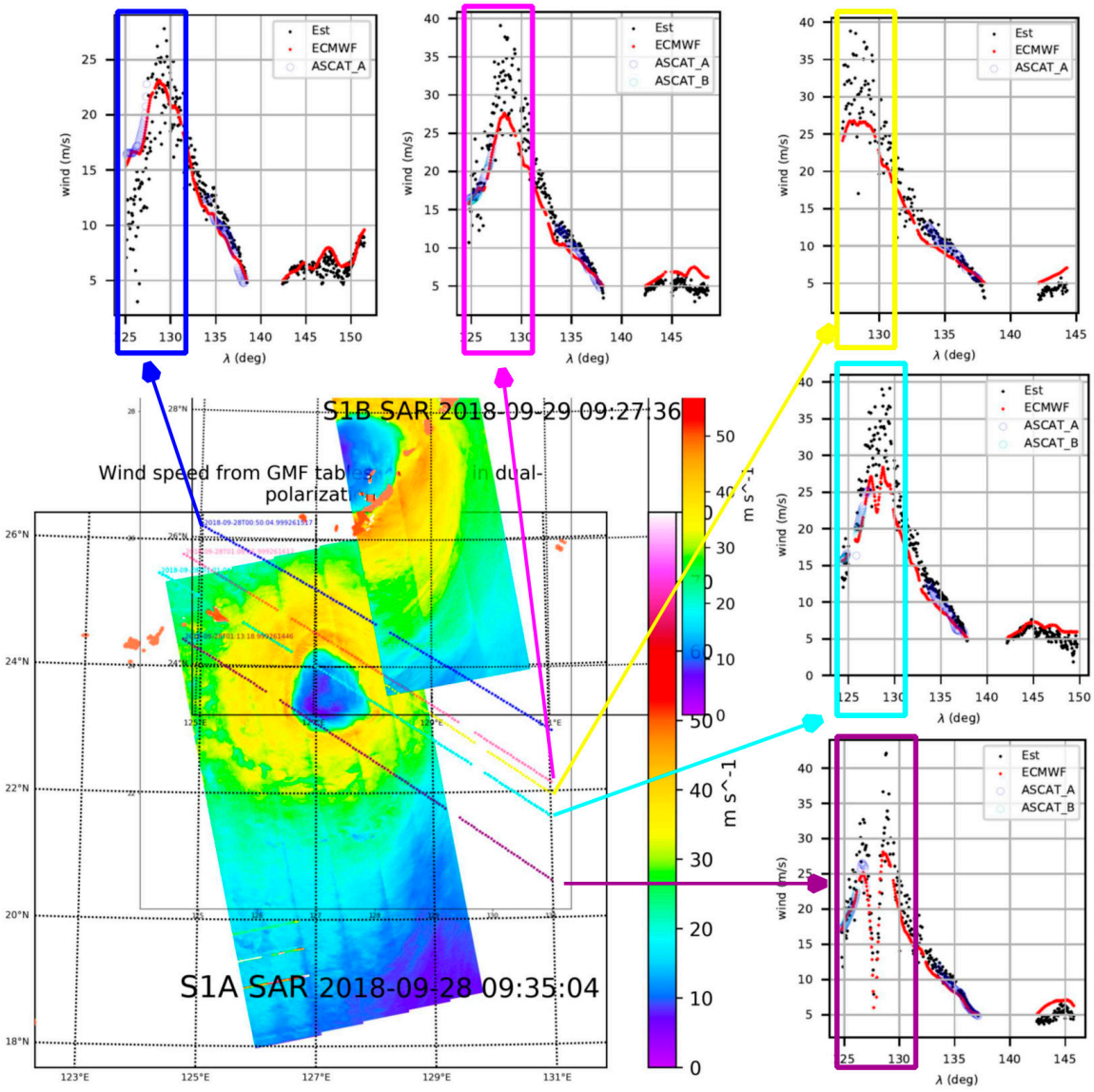

Figure 3. Sentinel-1A and -1B wind retrievals for Typhoon "Trami", acquired on Sep 28 9:35 (lower) and Sep 29 9:27 (upper) 2018, approximately 24 h apart (from https://cyclobs.ifremer.fr, 3 April 2021). The colored tracks are CYGNSS passes ~8 h before the first Synthetic Aperture Radar (SAR) wind field image (Sep 28, between 00:50 and 01:26) when the eye was further South. The CYGNSS wind retrievals for each of the tracks, estimated by A. Rius et al. [22], are shown in black dots ("Est" legend) in the panels surrounding the images. The red dots are for European Centre for Medium-Range Weather Forecasts (ECMWF) ERA-5 wind speeds interpolated to the CYGNSS tracks, and Advanced SCATterometer ASCAT-A/B are shown in blue circles when co-located.

Session 2: Data Products II

A CYGNSS L1 land product was developed by the University Corporation for Atmospheric Research (UCAR). This L1 land product [23] contains variables also found in the L1 ocean product, such as position, velocity, time, attitude, and antenna gain, while eliminates variables that were only applicable to ocean applications. The sandbox version of this product is available to all the Science Team members and includes almost all land bodies observed within CYGNSS coverage and a 50 km "skirt" of the ocean; however, very high-altitude regions, such as the Tibetan Plateau are not available due to on-board open loop tracker limitations.

In order to better assist with the CYGNSS wind speed product, several institutions including the National Oceanic and Atmospheric Administration (NOAA) have developed CYGNSS L2 wind speed products, which have been released through the PODAAC. As

compared to the original CYGNSS L2 wind speed product, the NOAA version is gridded into 25 × 25 km grid cells, and it uses a custom Geophysical Model Function (GMF) with a track-wise debiasing algorithm. At the time of this meeting, the presenters highlighted some of the minor changes going into v1.1 of the product, such as, e.g., resolving an issue with the star tracker flag, which led to an 18% increase in daily data on some dates. Most importantly, v1.1 of the CYGNSS-NOAA winds have led to improvements in wind speed retrievals within the cores of TCs. This product (Figure 4) was released through the PODAAC during the last fall, with data availability from March 2017 through the present [24].

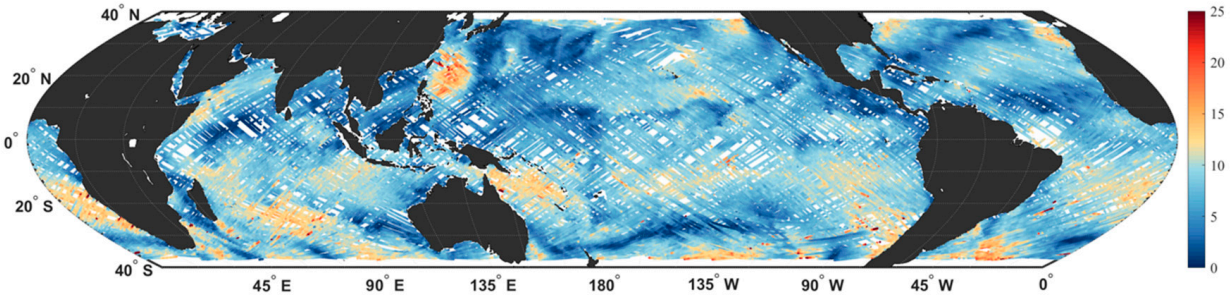

Figure 4. Full day of wind speed observations (m/s) on 30 August 2020 from the NOAA CYGNSS L2 Science Wind Speed 25-km v1.1 product.

An ocean surface heat flux product was released in August 2019, which combines CYGNSS L2 winds with reanalysis data from Modern-Era Retrospective analysis for Research and Applications (MERRA-2) in order to estimate the latent and sensible heat fluxes at each CYGNSS specular point [25]. An update of L2 CDR v1.0 of the CYGNSS ocean surface heat flux product was released in October 2020. As compared to the original version (Science Data Record (SDR) v1.0), the latest version of this product uses the CDR v1.0 L2 winds from CYGNSS, leading to a slightly improved performance as compared to buoy data and improved data availability for the Fully Developed Seas (FDS) versions of these products. Additionally, MERRA-2 variables are now matched in time and space to CYGNSS specular points using a tri-linear interpolation method rather than nearest neighbor, which has removed some biases and fixed issues near land. Similar to the CYGNSS-NOAA product, this product has been released through the PODAAC (Figure 5), with data availability from March 2017 through the present (with a 1-month data release latency) [26].

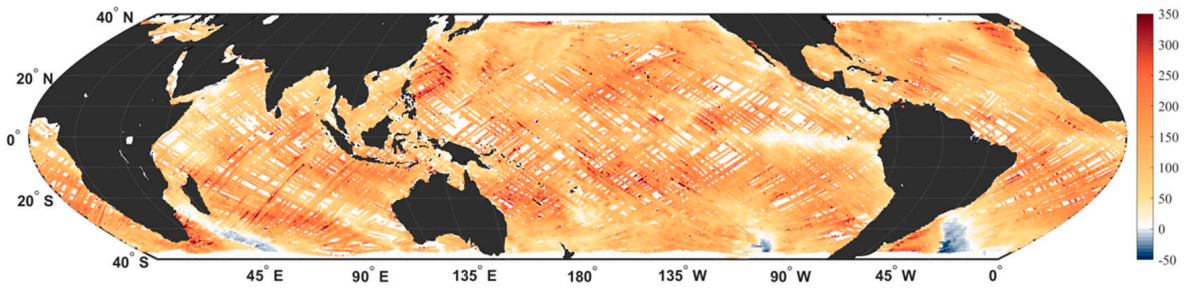

Figure 5. Full day of latent heat flux (W/m^2) observations on 30 August 2020 from the CYGNSS L2 Ocean Surface Heat Flux CDR v1.0 product.

NASA JPL serves as the primary data lead for CYGNSS within PODAAC, and continually provides updates to the CYGNSS Science Team regarding data publication. At the time of the meeting, the L1 ocean product remained the most popular CYGNSS product being downloaded, and the CYGNSS usage from October 2019 to May 2020 rebounded to pre-FTP retirement levels. It was also noted that by early 2021, cloud services for select datasets would become operational. Around the time of the meeting, PODAAC's web portal went through a revitalization to improve the user experience. This includes listing

all of the CYGNSS's data products on a single organized page, allowing users to have a better access to the CYGNSS's scientific data products.

2.2. Land Surfaces

The use of GNSS-R for land-surface applications requires additional considerations because the dielectric properties of this scattering medium have significantly more variability than that of the ocean surface. Here, we provide some of the latest findings of the CYGNSS mission, including key-results, discussions, and on-going research activities. At present, a significant number of researchers within the CYGNSS Science Team are working on land surface applications, which remain less explored than ocean products.

Session 3: Land Processes I

The first Land Processes Session consists of a series of presentations and discussions focusing on the use of CYGNSS data and observations related to (a) surface SMC estimation, (b) creation of dynamic inland water body masks, and (c) advancements in forward GNSS-R-related electromagnetic scattering and forward models. GNSS-R-like observations have been shown to be sensitive to changes in surface SMC [27–31] as well as the presence (or absence) of inland water bodies [32,33]. More recently, a 3 km CYGNSS Signal-to-Noise SNR-based surface SMC estimation approach was developed in [30], with results comparable to those by the NASA SMAP mission [34] and unbiased Root-Mean-Squared (ubRMSE) on the order of 0.045 m^3/m^3. Given this background, the following briefly summarizes the key finding from each of the session's presentations.

Forward scattering properties of Earth-reflected GNSS signals were evaluated over land surfaces. The CYGNSS End-to-End Simulator (E2ES) was updated. A GNSS-R model capable of evaluating both the incoherent and the coherent scattering terms was developed based on the Huygens–Kirchhoff principle [35]. Results demonstrated the impact of higher order Fresnel zones on the spatial resolution of GNSS-R over heterogeneous areas, showing "ringing" fluctuations in the reflected power near high-contrast boundaries.

An inland water body detection method was also presented during this session. The method [36] demonstrates the utility of ~2 years CYGNSS Level-1 Delay-Doppler Maps (DDM) to create [1,3] km water masks (Figure 6). Inland water surfaces at L-band are presumed smooth enough such that specular scattering is the dominant features in the observed DDM. Therefore, by deploying a DMM coherence persistence and detection method [30], mapping inlands becomes possible. The derived inland water body masks were qualitatively and quantitively compared to, and validated against, historical (30 years) water body occurrence maps by Pekel et al. [37]. False-positive areas were identified and removed via comparison to the Pekel occurrence maps, and examination of high-quality Digital Elevation Maps (DEM). Areas with persistent coherence, unknown water bodies, and exceptionally flat surfaces were also removed. The current analysis was based on ~2 years of CYGNSS observations. Additional investigation to identify false-positive and improve the overall detection method is required.

Russo et al. [38] outlined an entropy-based CYGNSS coherence detector—via eigenvalue decomposition of the DDMs—which, overall showed good agreement with wetland maps derived from Advanced Land Observing Satellite-2 (ALOS-2). However, the current method does not discriminate between open water and flooded vegetation and merits further investigation. Additionally, Russo et al. outlined a newly initiated research project with the ultimate goal of fusing CYGNSS-derived wetland with future wetland products from the NASA-ISRO Synthetic Aperture Radar (NISAR) mission. The primary motivation of this work was to develop the GNSS-R/SAR framework for future CYGNSS/NASA-ISRO (NISAR) activities.

Santi et al. [39,40] presented a series of Artificial Neural Network (ANN) implementations to use CYGNSS SNR observations to estimate various geophysical properties. Specifically, a multi-layer ANN model was trained to estimate AGB and tree height using CYGNSS SNR observations which uses training and reference data from the Geocarbon Pan-tropical forest maps by Avitabile et al. and tree height maps derived by the Geoscience

Laser Altimeter System (GLAS) instrument aboard the Ice, Cloud, and land Elevation Satellite (ICESat-1)

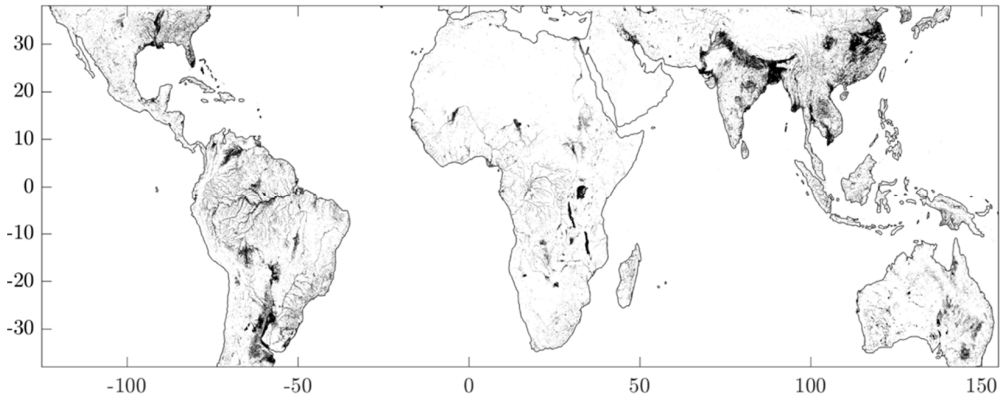

Figure 6. The 1−km land water body mask derived from CYGNSS L1 coherence-detection by M. Al-Khaldi et al. The map was generated using 1 year of CYGNSS data.

Recent theoretical developments in GNSS-R and scattering models over rough surfaces were also presented in this session [41]. Results and model validation efforts over the San Luis Valley, CO, showed promising matchups with the CYGNSS L1 Bistatic Radar Cross Section (BRCS). However, these studies also stressed the importance of accurately capturing and modeling multi-scale surface roughness and topographic effects.

This session also included several topics about retrieval and characterization of SMC and vegetation properties. A machine learning approach using random forest regression was presented to estimate SMC at a global scale [42]. The model was trained and generated using the reflectivity and relevant geophysical data layers, such as Normalized Difference Vegetation Index (NVDI) and DEM maps, along with SMC from the International Soil Moisture Network (ISMN). Results were validated over the Contiguous United States (CONUS) with consistent spatial patterns and magnitudes as those observed by the SMAP mission.

Similarly, by deriving a semi-analytical expression of vegetation transmissivity, and soil reflectivity, it was demonstrated how SMAP and CYGNSS observations can be concurrently leveraged to estimate either the Vegetation Optical Depth (VOD) and the SMC [43] (Figure 7). Additionally, a newly initiated study by Pu et al. sought to examine the effects of assimilation SMAP and CYGNSS SMC in near-surface weather forecasting models. This ongoing study showed that CYGNSS-derived SMC assimilation is on par with SMAP-based forecasts. However, further investigation is required to better quantify the added value by CYGNSS for SMC assimilation. Prior work by Pu et al. [44,45], however, demonstrates that strongly coupled land-surface assimilation frameworks which assimilate in situ, or SMAP, soil moisture can provide additional short-range and near-surface weather forecasting. The effects of CYGNSS SMC assimilation will be reported in future studies.

The use of CYGNSS high resolution ~3 km SMC maps was demonstrated by an experimental study supported by SERVIR [46]. This CYGNSS product, along with the ~3 km Land Information Systems (LIS) surface model, Integrated Multi-satellitE Retrievals for GPM (IMERG) rainfall, and Visible Infrared Imaging Radiometer Suite (VIRRS) vegetation information, was leveraged for locust monitoring applications in East Africa. SERVIR is a joint venture between NASA and the U.S. Agency for International Development. The SERVIR program is collaborating with regional entities in West and East Africa to evaluate the utility of Earth observations (EO), and their contribution to operational desert locust monitoring and tracking systems supported by the United Nations (UN) Food and Agriculture Organization (FAO).

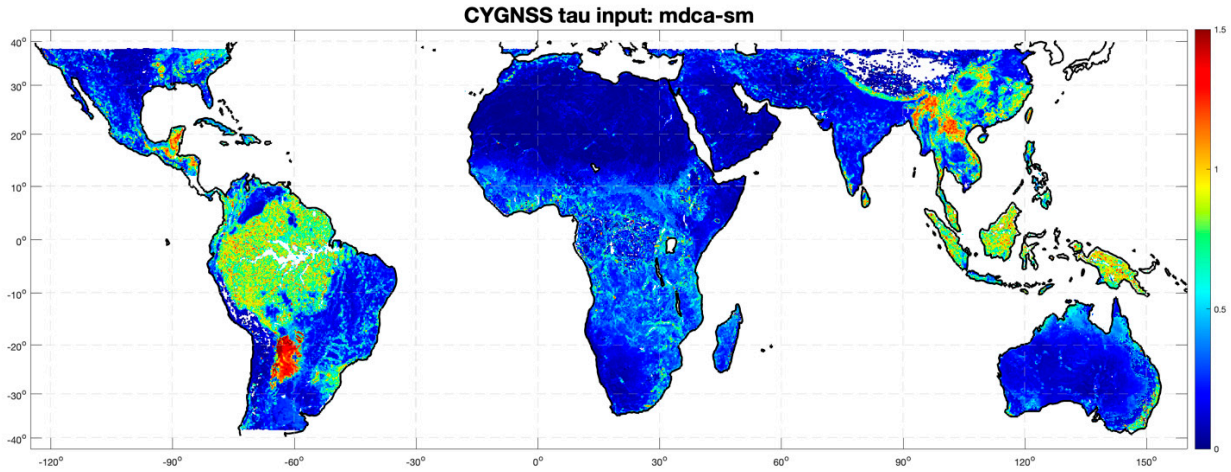

Figure 7. Example of CYGNSS-derived VOD by Xu et al.

Session 4: Land Processes II

Several studies have demonstrated the importance of coherent scattering of the GPS reflected signal over land [23,36,47–49]. In general, for coherent returns to exist, the GPS signal has to be reflected over very large flat areas with the surface RMSE height lower than ~10 cm at L-Band as presented in [50]. Recent analysis suggests that coherent returns are therefore mostly associated with the presence of inland water bodies [51,52]. This session will provide updates on current research using the SNR to detect inland water bodies. For land applications, surface roughness is a critical parameter for scattering models as detailed in the session. This surface roughness can be estimated using lidar airborne measurements [53]. Reflectometry has been used in various studies for land applications especially for retrieving SMC [53–56]. In this session, an update on the existing and potential calibration and validation sites for soil moisture applications is provided.

The first three presentations demonstrated the potential of the use of CYGNSS over land surfaces to detect and monitor water extent over short time scales [57]. The first method analyzed the distribution of time series of SNR for a given pixel to define dry and wet areas. With this method, a dynamic water extend mask can therefore be derived. Several case studies showed good correlation with rainfall events and the Pekel mask considered as the truth. Sensitivity of CYGNSS to water extent changes over short time scales was demonstrated by analyzing the spatial SNR variations with the seasonality of the Pascagoula River. Better detection results were obtained with a higher sampling rate. Finally, an investigation on the impact of land characteristics, such as SMC, surface water, topography and Vegetation Water Content (VWC) on the coherence of CYGNSS reflected signals was presented. The coherence was quantified using the tracked carrier phase from CYGNSS raw IF data. It was concluded that the coherent scattering term is most often present over inland water bodies.

The next topic of this session was assessing the impact of surface roughness, which is a critical parameter for correctly assessing the scattering of GNSS signals over land surfaces. A theoretical model was developed to decompose the surface into topography elevation and slopes, small-scale surface roughness, and surface correlation length. This new parametrization of the surface was tested using several classical forward-scattering models, including Geometrical Optics, Physical Optics, and Numerical Maxwell Model 3D (NMM3D). The modeled DDMs were then compared to CYGNSS-derived DDMs, showing a good agreement. In May 2020, experimental activities were performed along two cal/val sites over the San Luis Valley to characterize the small-scale surface roughness using lidar. Lidar-derived DEMs were generated at two different spatial resolutions, ~10 cm and ~30 cm.

The last three presentations dealt with actual and potential SMC cal/val sites for CYGNSS. First, an update was provided about the status of the SOILSCAPE in situ SMC

sensor networks, that were installed in two cal/val sites in the San Luis Valley. All sensors were shown to be working properly. Calibration of the SMC measurements is in process. New potential cal/val sites have been identified in the USA (Walnut Glutch, AZ, White Sands, NM) and in New Zealand. New Zealand cal/val sites are particularly of interest because the next generation GNSS-R receiver [58] is going to be installed on a regional Air New Zealand commercial aircraft to complement CYGNSS data, and to test this new receiver in preparation of a potential CYGNSS follow-on mission. An extensive analysis of the coverage provided by one Air New Zealand commercial aircraft was performed to identify the best cal/val site locations for SMC and wetlands studies. These locations were cross-compared with the CYGNSS coverage, showing several overlapping sites. This project will advance terrestrial and coastal retrievals, by generating long-term datasets with high spatial resolution and high spatiotemporal sampling. In addition, in support of this project, the deployment of the next-generation GNSS-R receiver on one Air New Zealand aircraft was simulated to get a better understanding of the differences of the reflected signal acquired on an aircraft as compared to a satellite. Flight paths, flight frequency, and GNSS-R coverage were analyzed. It was found to have promising coverage, except for some mountain regions in the South Island (Figure 8). Installing this new receiver on one aircraft will provide a large amount of information over both ocean and several land cover types. It was concluded that the extension to a fleet of regional aircrafts will generate an unprecedented GNSS-R scientifically valuable dataset.

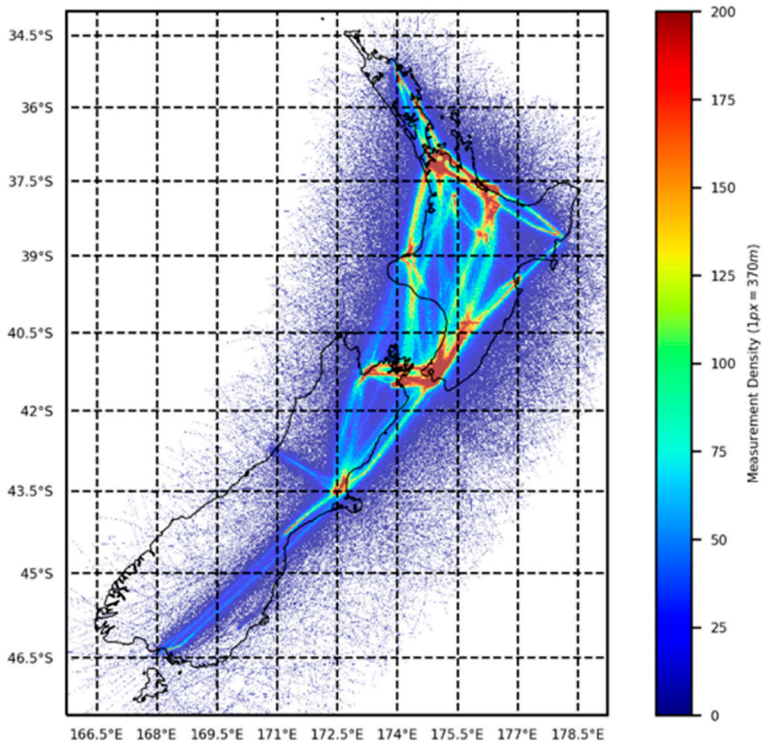

Figure 8. Simulated number of GNSS-R measurements over 1-year, considering just 1-single Air New Zealand aircraft by Linnabary et al.

2.3. Ocean Surfaces

The primary goal of the CYGNSS mission is to provide insight into the rapid intensification of TCs and to better measure their windspeeds. To this end, a number of studies since the mission's inception have focused on the application of CYGNSS data products to the study of TCs and tropical convection. Up until the release of the v3 winds data product, most of these studies have used simulated CYGNSS data for algorithm development. For example, Morris and Ruf developed parametric methods for filling in the gaps in the CYGNSS measurements [59], and for characterizing the size, structure, and strength of

a TC [60]. Several studies have used simulated CYGNSS winds to develop assimilation methods for improving tropical cyclone track and intensity forecasts [61–64]. Simulated CYGNSS winds have also been used to demonstrate convective activity monitoring [65]. With the successful development of the v3 winds data products, these studies have transitioned to the application of actual CYGNSS observations for applications such as improving storm center estimates [66] and developing a surface heat flux product [25]. Sessions 5–6 of the Science Team meeting focus on the progress made for ocean-based applications: TCs and other science applications, improving weather forecasts, and ocean altimetry.

Session 5: Altimetry and Tropical Cyclones and Tropical Convection I

A new approach has been developed to incorporate CYGNSS winds into storm surge models, using machine learning to determine a predictive model for CYGNSS winds in the future, based on Global Forecast System (GFS) forecast data and parametric model representation of the CYGNSS inner core TCs winds. The use of CYGNSS in conjunction with ancillary satellite data to measure diurnal wind variations was presented, including also initial results from a "rapid change detector" that is being developed to detect rapid changes to the wind field, which could be used to signal convective activity. Preliminary results of identifying early cyclogenesis from easterly waves using CYGNSS data were highlighted. The modality of the identification comes from the findings of increased L2 latent heat flux and surface wind speeds leading up to tropical cyclone genesis. An update on comparisons of CYGNSS MSSs to those derived from buoy measurements and a coupled atmospheric-wave-ocean model, confirmed the importance of including short wave contributions to the MSS in the models to match the observed MSS values. Validation efforts have been performed for the CYGNSS CDR v.1 products using data from microwave radiometers, including SMAP, WindSat and Advanced Microwave Scanning Radiometer (AMSR-2). A comparison of the wind speeds indicates that the CDR v.1 Young Sea/Limited Fetch (YSLF) winds are more accurate than the v2.1 wind speeds but still are poorly correlated to the other microwave radiometer wind speeds. The CYGNSS-NOAA wind speeds however, correlated well with the SMAP, AMSR2 and WindSat winds. Results of data assimilation of CYGNSS L1 DDMs into ECMWF background winds, where the resulting wind speeds, with and without the CYGNSS L1 DDM, were compared to scatterometer winds from the ASCAT-A, and B and the OceanSat Scatterometer (OSCAT).

The assimilation of the CYGNSS data (Figure 9) improved the ECMWF background at specular points predominantly for wind speeds < 15 m/s. Matched filter retrievals were applied for maximum CYGNSS TCs winds, using the Willoughby–Darling–Rahn model [67]. After eliminating storms that violated the model's assumptions, good results were obtained for the matched filter output. An update of CYGNSS L1 data for ocean altimetry was presented, showing a number of improvements and corrections, including waveform pre-processing, delay compensation, and re-tracking. New results were presented for a case study in the Caribbean. Finally, an overview of several CYGNSS-based altimetry methods was presented, showing an accuracy on the order of several meters. Future improvements are likely to be achieved in accounting better for tides, and ionosphere and troposphere delays.

Session 6: Tropical Cyclones and Tropical Convection II

The final session of the June 2020 CYGNSS Science Team meeting focused on the use of the L2 wind speed products for improving forecasts and wind field analyses of TCs and tropical convection. CYGNSS provides wind speed data that can be used for storm surge predictions, which is a major source of destruction for communities lying in the paths of a storm. Simulations showed the storm surge from the Hurricane Harvey (2017), which were driven in part by wind speed observations from CYGNSS. Efforts were performed to diagnose the structure of TCs' wind fields using the CYGNSS wind speed observations and found that, given good quality data from CYGNSS, the size of the wind field can be determined. A methodology for creating storm wind fields that move with the storm over time was also presented (Figure 10). These datasets are available in PODAAC, alongside other CYGNSS products [68].

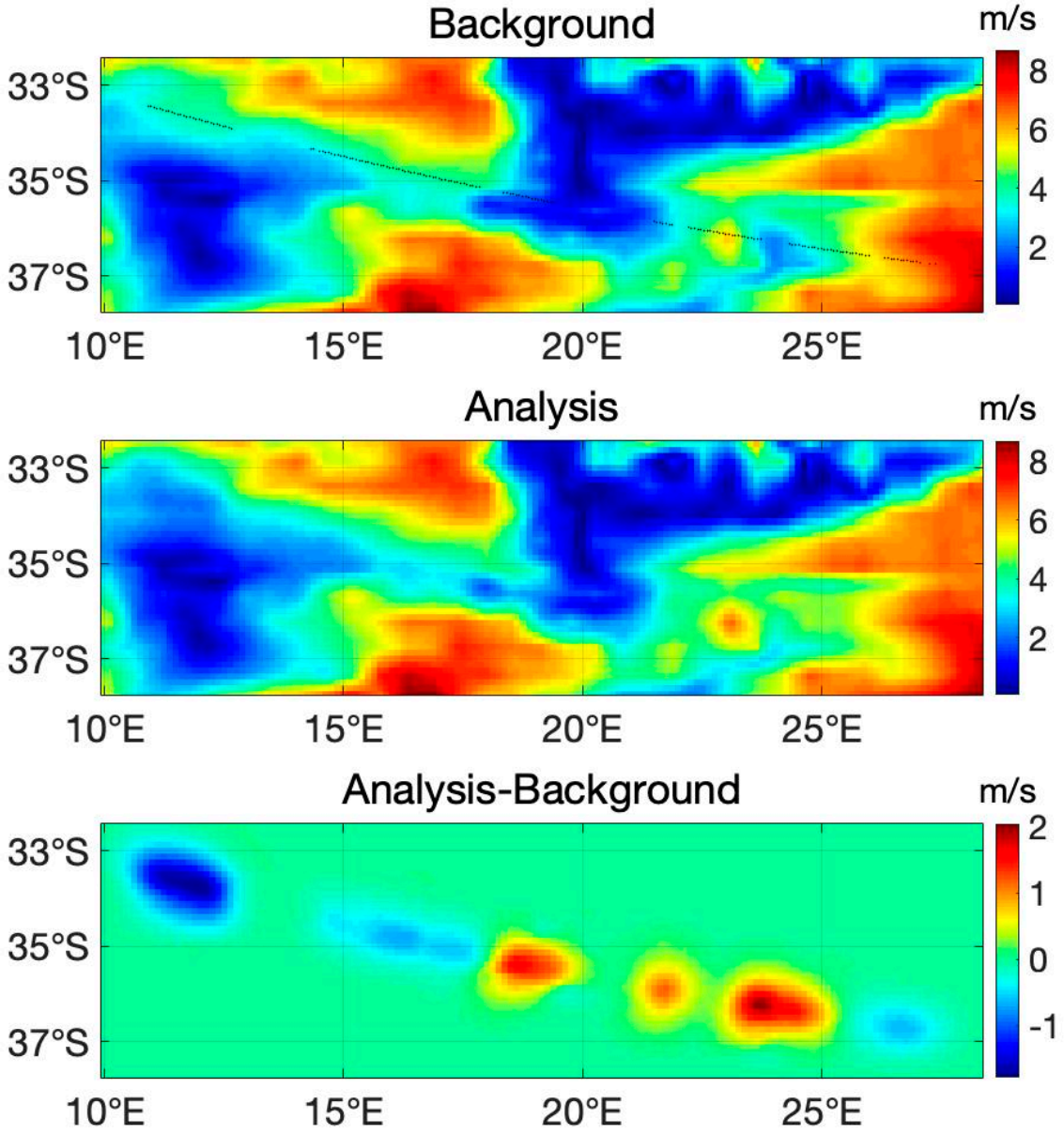

Figure 9. Assimilating CYGNSS DDMs into ECMWF background winds to improve surface wind forecasts: [**top**] demonstrating the ECMWF background at 150 km resolution, [middle] analysis field with the DDM assimilation, and [**bottom**] the difference between the two. Image by F. Huang et al.

Apart from analysis of storm wind fields, the observations from CYGNSS are also being used to improve weather forecasts. Efforts to improve the initialization of weather model simulations with CYGNSS observations were presented, including also information about where CYGNSS improves the forecasts of TCs. Throughout the session, team members compared techniques for quality control and optimal ingestion of wind speed data from CYGNSS.

CYGNSS is also playing a role in studies of tropical convection, where other observations suffer in heavy precipitation. Simulations of tropical convection with a coupled atmosphere, ocean, wave model were described, along with a comparison of simulated winds with those observed by CYGNSS. A number of on-going investigations examined CYGNSS observations near tropical oceanic thunderstorms, including an examination of the characteristics of the data in storms with and without lightning [69]. The importance of wind-driven fluxes on the Madden Julian Oscillation (MJO), using CYGNSS data was high-

lighted [70]. Finally, it is worth highlighting that several team members are using CYGNSS data to study the processes of air-sea interaction in weather and climate science [71].

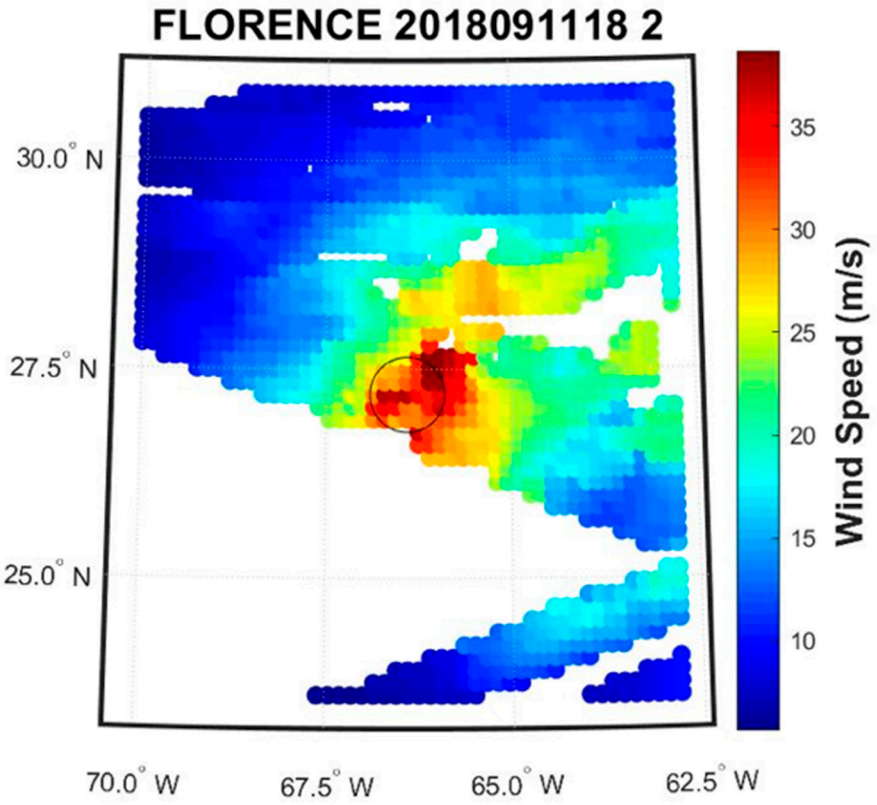

Figure 10. CYGNSS-derived wind speed retrievals over the Hurricane Florence by D. Mayers et al.

3. Conclusions and Final Remarks

NASA's CYGNSS 8 microsatellite-constellation is the first-ever operational GNSS-R mission, revolutionizing several scientific fields within our community, and attracting new members from different communities such as microwave radiometry and SAR. The number of GNSS-R scientific publications within our community continues to increase significantly thanks to the open-access CYGNSS products available at the PODAAC. This was a nice start, but the CYGNSS Science Team is a dynamic community always looking to improve products and apply them to new scientific applications. In this scenario, around 50% of the Science Team members are now involved with applications over land surfaces, including SMC, AGB, and water surface. The key enabling events were improving calibration procedures, product spatial resolution (e.g., reducing date integration to 0.5 s from 1 s), geolocation, metadata quality, and a more agile web for downlinking data.

The recent mission extension by NASA will enable the continuation of investigations by the CYGNSS Science Team. We will continue to contribute to the wider remote sensing community with our new and novel results, with the objective of advancing our understanding of key dynamic processes over the Earth's surface. With this article, we welcome new members to participate in the CYGNSS mission.

Author Contributions: Conceptualization, C.R. and H.C.-L.; methodology, C.R. and H.C.-L.; writing—original draft preparation, C.R., H.C.-L., R.A., A.B., J.A.C., M.M. and A.W.; writing—review and editing, C.R., H.C.-L., R.A., A.B., J.A.C., M.M. and A.W.; visualization, C.R. and H.C.-L.; supervision, C.R. and H.C.-L.; project administration, C.R.; funding acquisition, C.R. All authors have read and agreed to the published version of the manuscript.

Funding: This research was supported in part by the NASA Science Mission Directorate contract NNL13AQ00C with the University of Michigan.

Institutional Review Board Statement: Not applicable.

Informed Consent Statement: Not applicable.

Conflicts of Interest: The authors declare no conflict of interest.

Acronyms

Above Ground Biomass (AGB)
Advanced Land Observing Satellite-2 (ALOS-2)
Advanced Microwave Scanning Radiometer (AMSR-2)
Advanced SCATterometer (ASCAT)
Artificial Neural Network (ANN)
Bistatic Radar Cross Section (BRCS)
Climate Data Record (CDR)
Contiguous United States (CONUS)
Cyclone Global Navigation Satellite System (CYGNSS)
Delay Doppler Map (DDM)
Delay Doppler Mapping Instrument (DDMI)
Digital Elevation Model (DEM)
Disaster Monitoring System-1 (DMC-1)
Earth Observation (EO)
Earth System Science Pathfinder (ESSP)
End-to-End Simulator (E2ES)
European Centre for Medium-Range Weather Forecasts (ECMWF)
European Space Agency (ESA)
Flight Model (FM)
Food and Agriculture Organization (FAO)
Fully Developed Seas (FDS)
Physical Oceanography Distributed Active Archive Center (PODAAC)
Geophysical Model Function (GMF)
Global Forecast System (GFS)
Global Navigation Satellite Systems (GNSS)
Global Positioning System (GPS)
Institute of Space Sciences (ICE)
Institute of Space Studies of Catalonia (IEEC)
Intermediate Frequency (IF)
International Soil Moisture Network (ISMN)
Jet Propulsion Laboratory (JPL)
Land Information Systems (LIS)
Low Earth Orbit (LEO)
Madden Julian Oscillation (MJO)
Maxwell Model 3D (NMM3D)
Mean-Square Slope (MSS)
Modern-Era Retrospective analysis for Research and Applications (MERRA-2)
Multi-satellitE Retrievals for GPM (IMERG)
National Aeronautics and Space Administration (NASA)
NASA-ISRO (NISAR)
National Oceanic and Atmospheric Administration (NOAA)
Normalized Difference Vegetation Index (NVDI)
OceanSat Scatterometer (OSCAT)
Pseudo-Random Noise (PRN)Research Opportunities in Space and Earth Science (ROSES)
Science Data Record (SDR)
Signal-to-Noise Ratio (SNR)
Soil Moisture Active Passive (SMAP)
Soil Moisture Content (SMC)
Soil Moisture Ocean Salinity (SMOS)Space-borne Imaging Radar-C (SIR-C)

Synthetic Aperture Radar (SAR)
TechDemoSat-1 (TDS-1)
Tropical Cyclone (TC)
United Kingdom (UK)United Nations (UN)
University Corporation for Atmospheric Research (UCAR)
University of Michigan (UM)
Vegetation Optical Depth (VOD)
Vegetation Water Content (VWC)
Visible Infrared Imaging Radiometer Suite (VIRRS)
Wave-Watch 3 (WW3)
Young Sea/Limited Fetch (YSLF)

References

1. Ruf, C.; Unwin, M.; Dickinson, J.; Rose, R.; Rose, D.; Vincent, M.; Lyons, A. CYGNSS: Enabling the Future of Hurricane Prediction [Remote Sensing Satellites]. *IEEE Geosci. Remote Sens. Mag.* **2013**, *1*, 52–67. [CrossRef]
2. Ruf, C.; Chang, P.S.; Clarizia, M.P.; Gleason, S.; Jelenak, Z.; Majumdar, S.; Morris, M.; Murray, J.; Musko, S.; Posselt, D.; et al. *CYGNSS Handbook. Cyclone Global Navigation Satellite System*; Michigan Publishing: Ann Arbor, MI, USA, 2016. Available online: https://clasp-research.engin.umich.edu/missions/cygnss/reference/cygnss-mission/CYGNSS_Handbook_April2016.pdf (accessed on 2 February 2021).
3. Ruf, C.; Atlas, R.; Chang, P.S.; Clarizia, M.P.; Garrison, J.L.; Gleason, S.; Katzberg, S.J.; Jelenak, Z.; Johnson, J.T.; Majumdar, S.J.; et al. New Ocean Winds Satellite Mission to Probe Hurricanes and Tropical Convection. *Bull. Am. Meteorol. Soc.* **2015**, *97*, 385–395. [CrossRef]
4. Ruf, C.; Cardellach, E.; Clarizia, M.P.; Galdi, C.; Gleason, S.T.; Paloscia, S. Foreword to the Special Issue on Cyclone Global Navigation Satellite System (CYGNSS) Early on Orbit Performance. *IEEE J. Sel. Top. Appl. Earth Obs. Remote Sens.* **2019**, *12*, 3–6. [CrossRef]
5. Ruf, C.; Asharaf, S.; Balasubramaniam, R.; Gleason, S.; Lang, T.; McKague, D.; Twigg, D.; Waliser, D. In-Orbit Performance of the Constellation of CYGNSS Hurricane Satellites. *Bull. Am. Meteorol. Soc.* **2019**, *100*, 2009–2023. [CrossRef]
6. Carreno-Luengo, H.; Luzi, G.; Crosetto, M. Sensitivity of CYGNSS Bistatic Reflectivity and SMAP Microwave Radiometry Brightness Temperature to Geophysical Parameters over Land Surfaces. *IEEE J. Sel. Top. Appl. Earth Obs. Remote Sens.* **2019**, *12*, 107–122. [CrossRef]
7. Carreno-Luengo, H.; Luzi, G.; Crosetto, M. Above-Ground Biomass Retrieval over Tropical Forests: A Novel GNSS-R Approach with CyGNSS. *Remote Sens.* **2020**, *12*, 1368. [CrossRef]
8. Warnock, A.; Ruf, C. Response to Variations in River Flowrate by a Spaceborne GNSS-R River Width Estimator. *Remote Sens.* **2019**, *11*, 2450. [CrossRef]
9. Martin-Neira, M. A Passive Reflectometry and Interferometry System (PARIS): Application to Ocean Altimetry. *ESA J.* **1993**, *17*, 331–355.
10. Lowe, S.T.; Labrecque, J.L.; Zuffada, C.; Romans, L.J.; Young, L.E.; Hajj, G.A. First spaceborne observation of an Earth-reflected GPS signal. *Radio Sci.* **2002**, *37*, 7–1–7–28. [CrossRef]
11. Gleason, S.; Hodgart, S.; Sun, Y.; Gommenginger, C.; Mackin, S.; Adjrad, M.; Unwin, M. Detection and Processing of bistatically reflected GPS signals from low Earth orbit for the purpose of ocean remote sensing. *IEEE Trans. Geosci. Remote Sens.* **2005**, *43*, 1229–1241. [CrossRef]
12. Unwin, M.; Jales, P.; Blunt, P.; Duncan, S. Preparation for the First Flight of SSTL's Next Generation Space GNSS Receivers. In Proceedings of the 6th ESA/European Workshop Satellite NAVITEC GNSS Signals Signal Processor, Noordwijk, The Netherlands, 5–7 December 2012; pp. 1–6.
13. Carreno-Luengo, H.; Lowe, S.; Zuffada, C.; Esterhuizen, S.; Oveisgharan, S. Spaceborne GNSS-R from the SMAP Mission: First Assessment of Polarimetric Scatterometry over Land and Cryosphere. *Remote Sens.* **2017**, *9*, 362. [CrossRef]
14. CYGNSS Mission Teams. Available online: https://clasp-research.engin.umich.edu/missions/cygnss/mission-teams.php (accessed on 3 March 2021).
15. Ruf, C.; Gleason, S.; Jelenak, Z.; Katzberg, S.; Ridley, A.; Rose, R.; Scherrer, J.; Zavorotny, V. The CYGNSS Nanosatellite Constellation Hurricane Mission. In Proceedings of the IEEE International Geoscience and Remote Sensing Symposium, Munich, Germany, 22–27 July 2012; pp. 214–216.
16. Dickinson, J.; Ruf, C.; Rose, R.; Ridley, A.; Walls, B. CYGNSS: The Cyclone Global Navigation Satellite System's CubeSat Foundations. In Proceedings of the 12th Annual Joint Agency Commercial Imagery Evaluation (JACIE) Workshop, St. Louis, MO, USA, 16–18 April 2013.
17. Ruf, C.; Lyons, A.; Ward, A. NASA Intensifies Hurricane Studies with CYGNSS. *Earth Obs. NASA* **2013**, *25*, 12–21.
18. Gleason, S.; Ruf, C.; Clarizia, M.P.; O'Brien, A. Calibration and Unwrapping of the Normalized Scattering Cross Section for the Cyclone Global Navigation Satellite System (CYGNSS). *IEEE Trans. Geosci. Remote Sens.* **2016**, *54*, 2495–2509. [CrossRef]
19. CYGNSS Data Products. Available online: https://clasp-research.engin.umich.edu/missions/cygnss/data-products.php (accessed on 3 March 2021).

20. Ruf, C. Mission Update. In Proceedings of the CYGNSS Science Team Meeting, Ann Arbor, MI, USA, 6 June 2020.
21. Wang, T.; Zavorotny, V.U.; Johnson, J.; Yi, Y.; Ruf, C.; Gleason, S.; McKague, D.; Hwang, P.; Rogers, E.; Chen, S.; et al. Improvement of CYGNSS Level 1 Calibration Using Modeling and Mesurements of Ocean Surface Mean Square Slope. In Proceedings of the 2020 IEEE International Geoscience and Remote Sensing Symposium (IGARSS), Waikoloa, HI, USA, 26 September–2 October 2020; pp. 5909–5912.
22. Cardellach, E.; Nan, Y.; Li, W.; Padulles, R.; Ribo, S.; Rius, A. Variational Retrievals of High Winds Using Uncalibrated CYGNSS Observables. *Remote Sens.* **2020**, *12*, 3930. [CrossRef]
23. Gleason, S.; O'Brien, A.; Russel, A.; Al-Khaldi, M.M.; Johnson, J.T. Geolocation, Calibration and Surface Resolution of CYGNSS GNSS-R Land Observations. *Remote Sens.* **2020**, *12*, 1317. [CrossRef]
24. *NOAA CYGNSS Level 2 Science Wind Speed 25-km Product*, Version 1.1 ed; PO.DAAC: Pasadena, CA, USA, 2020. Available online: https://doi.org/10.5067/CYGNN-22511 (accessed on 21 March 2021).
25. Crespo, J.A.; Posselt, D.J.; Asharaf, S. CYGNSS Surface Heat Flux Product Development. *Remote Sens.* **2019**, *11*, 2294. [CrossRef]
26. *CYGNSS Level 2 Ocean Surface Heat Flux Climate Data Record*, Version 1.0 ed; PO.DAAC: Pasadena, CA, USA. Available online: https://doi.org/10.5067/CYGNS-C2H10 (accessed on 21 March 2021).
27. Ruf, C.S.; Chew, C.; Lang, T.; Morris, M.G.; Nave, K.; Ridley, A.; Balasubramaniam, R. A New Paradigm in Earth Environmental Monitoring with the CYGNSS Small Satellite Constellation. *Sci. Rep.* **2018**, *8*, 8782. [CrossRef]
28. Rodriguez-Alvarez, N.; Bosch-Lluis, X.; Camps, A.; Vall-Llossera, M.; Valencia, E.; Marchan-Hernandez, J.F.; Ramos-Perez, I. Soil Moisture Retrieval Using GNSS-R Techniques: Experimental Results Over a Bare Soil Field. *IEEE Trans. Geosci. Remote Sens.* **2009**, *47*, 11. [CrossRef]
29. Camps, A.; Park, H.; Pablos, M.; Foti, G.; Gommenginger, C.P.; Liu, P.-W.; Judge, J. Sensitivity of GNSS-R Spaceborne Observations to Soil Moisture and Vegetation. *IEEE J. Sel. Top. Appl. Earth Obs. Remote Sens.* **2016**, *9*, 4730–4742. [CrossRef]
30. Chew, C.; Shah, R.; Zuffada, C.; Hajj, G.; Masters, D.; Mannucci, A.J. Demonstrating Soil Moisture Remote Sensing with Observations from the UK TechDemoSat-1 Satellite Mission. *Geophys. Res. Lett.* **2016**, *43*, 3317–3324. [CrossRef]
31. Eroglu, O.; Kurum, M.; Boyd, D.; Gurbuz, A.C. High Spatio-Temporal Resolution CYGNSS Soil Moisture Estimates Using Artificial Neural Networks. *Remote Sens.* **2019**, *11*, 2272. [CrossRef]
32. Nghiem, S.V.; Zuffada, C.; Shah, R.; Chew, C.; Lowe, S.T.; Mannucci, A.J.; Cardellach, E.; Brakenridge, G.R.; Geller, G.; Rosenqvist, A. Wetland Dynamics Monitoring with Global Navigation Satellite System Reflectometry. *AGU Earth Space Sci.* **2017**, *4*, 16–39. [CrossRef]
33. Zuffada, C.; Chew, C.; Nghiem, S.V. GNSS-R Algorithms for Wetlands Observations. In Proceedings of the 2017 IEEE International Geoscience and Remote Sensing Symposium (IGARSS), Fort Worth, TX, USA, 23–28 July 2017; pp. 1126–1129.
34. Entekhabi, D.; Njoku, E.G.; O'Neill, P.E.; Kellogg, K.H.; Crow, W.T.; Edelstein, W.N.; Entin, J.K.; Goodman, S.D.; Jackson, T.J.; Johnson, J.; et al. The Soil Moisture Active Passive (SMAP) Mission. *Proc. IEEE* **2010**, *98*, 704–716. [CrossRef]
35. Carreno-Luengo, H.; Ruf, C.; Warnock, A.; Brunner, K. Investigating the Impact of Coherent and Incoherent Scattering Terms in GNSS-R Delay Doppler Maps. In Proceedings of the 2020 IEEE International Geoscience and Remote Sensing Symposium (IGARSS), Waikoloa, HI, USA, 26 September–2 October 2020; pp. 6202–6205.
36. Al-Khaldi, M.M.; Johnson, J.T.; Gleason, S.; Loria, E.; O'Brien, A.J.; Yi, Y. An Algorithm for Detecting Coherence in Cyclone Global Navigation Satellite System Mission Level-1 Delay-Doppler Maps. *IEEE Trans. Geosci. Remote Sens.* **2021**, *59*, 4454–4463. [CrossRef]
37. Pekel, J.-F.; Cottam, A.; Gorelick, N.; Belward, A.S. High-resolution mapping of global surface water and its long-term changes. *Nature* **2016**, *540*, 418–422. [CrossRef]
38. Russo, I.M.; di Bisceglie, M.; Galdi, C.; Lavalle, M.; Zuffada, C. Wave Coherence in GNSS Reflectometry: A Signal Processing Point of View. In Proceedings of the 2020 IEEE International Geoscience and Remote Sensing Symposium (IGARSS), Waikoloa, Hawaii, USA, 26 September–2 October 2020; pp. 6214–6217.
39. Santi, E.; Paloscia, S.; Pettinato, S.; Fontanelli, G.; Clarizia, M.P.; Comite, D.; Dente, L.; Guerriero, L.; Pierdicca, N.; Floury, N. Remote Sensing of Forest Biomass Using GNSS Reflectometry. *IEEE J. Sel. Top. Appl. Earth Obs. Remote Sens.* **2020**, *13*, 2351–2368. [CrossRef]
40. Santi, E.; Pettinato, S.; Paloscia, S.; Clarizia, M.P.; Dente, L.; Guerriero, L.; Comite, D.; Pierdicca, N. Soil Moisture and Forest Biomass retrieval on a global scale by using CyGNSS data and Artificial Neural Networks. In Proceedings of the IEEE International Geoscience and Remote Sensing Symposium, Waikoloa, HI, USA, 26 September–2 October 2020; pp. 214–216.
41. Campbell, J.D.; Melebari, A.; Moghaddam, M. Modeling the Effects of Topography on Delay-Doppler Maps. *IEEE J. Sel. Top. Appl. Earth Obs. Remote Sens.* **2020**, *13*, 1740–1751. [CrossRef]
42. Senyurek, V.; Lei, F.; Boyd, D.; Gurbuz, A.C.; Kurum, M.; Moorhead, R. Evaluations of Machine Learning-Based CYGNSS Soil Moisture Estimates against SMAP Observations. *Remote Sens.* **2020**, *12*, 3503. [CrossRef]
43. Yueh, S.H.; Shah, R.; Chaubell, M.J.; Hayashi, A.; Xu, X.; Colliander, A. A Semiempirical Modeling of Soil Moisture, Vegetation, and Surface Roughness Impact on CYGNSS Reflectometry Data. *IEEE Trans. Geosci. Remote Sens.* **2020**. [CrossRef]
44. Lin, L.; Pu, Z. Improving Near-Surface Short-Range Weather Forecasts Using Strongly Coupled Land–Atmosphere Data Assimilation with GSI-EnKF. *Mon. Weather Rev.* **2020**, *148*, 2863–2888. [CrossRef]
45. Lin, L.-F.; Pu, Z. Examining the Impact of SMAP Soil Moisture Retrievals on Short-Range Weather Prediction under Weakly and Strongly Coupled Data Assimilation with WRF-Noah. *Mon. Weather Rev.* **2019**, *147*, 4345–4366. [CrossRef]

46. Chew, C.C.; Small, E.E. Soil Moisture Sensing Using Spaceborne GNSS Reflections: Comparison of CYGNSS Reflectivity to SMAP Soil Moisture. *Geophys. Res. Lett.* **2018**, *45*, 4049–4057. [CrossRef]
47. Park, J.; Johnson, J.T.; O'Brien, A.; Lowe, S.T. An Examination of TDS-1 GNSS-R Returns over Land Surfaces. In Proceedings of the URSI Radio Science Meeting, Pasadena, CA, USA, 6–9 January 2016.
48. Loria, E.; O'Brien, A.; Gupta, I.J. Detection and Separation of Coherent Reflections in GNSS-R Measurements Using CYGNSS Data. In Proceedings of the IEEE International Geoscience and Remote Sensing Symposium, Valencia, Spain, 22–27 July 2018; pp. 3995–3998.
49. Dong, Z.; Jin, S. Evaluation of the Land GNSS-Reflected DDM Coherence on Soil Moisture Estimation from CYGNSS Data. *Remote Sens.* **2021**, *13*, 570. [CrossRef]
50. Balakhder, A.M.; Al-Khaldi, M.M.; Johnson, J.T. On the Coherency of Ocean and Land Surface Specular Scattering for GNSS-R and Signals of Opportunity Systems. *IEEE Trans. Geosci. Remote Sens.* **2019**, *57*, 10426–10436. [CrossRef]
51. Al-Khaldi, M.M.; Johnson, J.T.; Gleason, S.; Chew, C.C.; Gerlein-Safdi, C.; Shah, R.; Zuffada, C. Inland Water Body Mapping Using CYGNSS Coherence Detection. *IEEE Trans. Geosci. Remote Sens.* **2021**. [CrossRef]
52. Gerlein-Safdi, C.; Ruf, C.S. A CYGNSS-Based Algorithm for the Detection of Inland Waterbodies. *Geophys. Res. Lett.* **2019**, *46*, 12065–12072. [CrossRef]
53. Turner, R.; Panciera, R.; Tanase, M.A.; Lowell, K.; Hacker, J.M.; Walker, J.P. Estimation of Soil Surface Roughness of Agricultural Soils Using Airborne LiDAR. *Remote Sens. Environ.* **2014**, *140*, 107–117. [CrossRef]
54. Kim, H.; Lakshmi, V. Use of Cyclone Global Navigation Satellite System (CYGNSS) Observations for Estimation of Soil Moisture. *Geophys. Res. Lett.* **2018**, *45*, 8272–8282. [CrossRef]
55. Al-Khaldi, M.M.; Johnson, J.T.; O'Brien, A.J.; Balenzano, A.; Mattia, F. Time-Series Retrieval of Soil Moisture Using CYGNSS. *IEEE Trans. Geosci. Remote Sens.* **2019**, *57*, 4322–4331. [CrossRef]
56. Clarizia, M.P.; Pierdicca, N.; Costantini, F.; Floury, N. Analysis of CYGNSS Data for Soil Moisture Retrieval. *IEEE J. Sel. Top. Appl. Earth Obs. Remote Sens.* **2019**, *12*, 2227–2235. [CrossRef]
57. Gerlein-Safdi, C.; Ruf, C. CYGNSS Constellation Provides New Insight on Tropical Wetlands Dynamics. In Proceedings of the ESA Annual Meeting, ESA-ESTEC, Noordwijk, The Netherlands, 3–6 August 2020.
58. Ruf, C.; Backhus, R.; Butler, T.; Chen, C.C.; Gleason, S.; Loria, E.; McKague, D.; Miller, R.; O'Brien, A.; van Nieuwstadt, L. Next Generation GNSS-R Instrument. In Proceedings of the 2020 IEEE International Geoscience and Remote Sensing Symposium, Waikoloa, HI, USA, 26 September–2 October 2020; pp. 3353–3356.
59. Morris, M.; Ruf, C.S. Determining Tropical Cyclone Surface Wind Speed Structure and Intensity with the CYGNSS Satellite Constellation. *J. Appl. Meteorol. Clim.* **2017**, *56*, 1847–1865. [CrossRef]
60. Morris, M.; Ruf, C.S. Estimating Tropical Cyclone Integrated Kinetic Energy with the CYGNSS Satellite Constellation. *J. Appl. Meteorol. Clim.* **2017**, *56*, 235–245. [CrossRef]
61. Zhang, S.; Pu, Z.; Posselt, D.J.; Atlas, R. Impact of CYGNSS Ocean Surface Wind Speeds on Numerical Simulations of a Hurricane in Observing System Simulation Experiments. *J. Atmos. Ocean. Technol.* **2017**, *34*, 375–383. [CrossRef]
62. Annane, B.; McNoldy, B.; Leidner, S.M.; Hoffman, R.; Atlas, R.; Majumdar, S.J. A Study of the HWRF Analysis and Forecast Impact of Realistically Simulated CYGNSS Observations Assimilated as Scalar Wind Speeds and as VAM Wind Vectors. *Mon. Weather Rev.* **2018**, *146*, 2221–2236. [CrossRef]
63. Leidner, S.M.; Annane, B.; McNoldy, B.; Hoffman, R.; Atlas, R. Variational Analysis of Simulated Ocean Surface Winds from the Cyclone Global Navigation Satellite System (CYGNSS) and Evaluation Using a Regional OSSE. *J. Atmos. Ocean. Technol.* **2018**, *35*, 1571–1584. [CrossRef]
64. Cui, Z.; Pu, Z.; Tallapragada, V.; Atlas, R.; Ruf, C.S. A Preliminary Impact Study of CYGNSS Ocean Surface Wind Speeds on Numerical Simulations of Hurricanes Harvey and Irma (2017). *Geophys. Res. Lett.* **2019**, *46*, 2984–2992. [CrossRef]
65. Park, J.; Johnson, J.T.; Yi, Y.; O'Brien, A.J. Using "Rapid Revisit" CYGNSS Wind Speed Measurements to Detect Convective Activity. *J. Sel. Top. Appl. Earth Obs. Remote Sens.* **2019**, *12*, 98–106. [CrossRef]
66. Mayers, D.; Ruf, C. Tropical Cyclone Center Fix Using CYGNSS Winds. *J. Appl. Meteorol. Clim.* **2019**, *58*, 1993–2003. [CrossRef]
67. Huang, F.; Garrison, J.L.; Leidner, S.M.; Annane, B.; Hoffman, R.N.; Grieco, G.; Stoffelen, A. A Forward Model for Data Assimilation of GNSS Ocean Reflectometry Delay-Doppler Maps. *IEEE Trans. Geosci. Remote Sens.* **2020**, *59*, 2643–2656. [CrossRef]
68. *CYGNSS Level 3 Storm Centric Grid Science Data Record*, Version 1.0 ed; PO.DAAC: Pasadena, CA, USA. Available online: https://doi.org/10.5067/CYGNS-L3S10 (accessed on 21 March 2021).
69. Lang, T. Comparing Winds Near Tropical Oceanic Precipitation Systems with and without Lightning. *Remote Sens.* **2020**, *12*, 3968. [CrossRef]
70. Bui, H.X.; Maloney, E.D.; Dellaripa, E.M.R.; Singh, B. Wind Speed, Surface Flux, and Intraseasonal Convection Coupling from CYGNSS Data. *Geophys. Res. Lett.* **2020**, *47*, e2020GL090376. [CrossRef]
71. Crespo, J.A.; Naud, C.M.; Posselt, D.J. CYGNSS Observations and Analysis of Low-Latitude Extratropical Cyclones. *J. Appl. Meteorol. Clim.* **2021**, *60*, 527–541. [CrossRef]